

Spleen-derived lipocalin-2 in the portal vein regulates Kupffer cells activation and attenuates the development of liver fibrosis in mice

Tomonori Aoyama¹, Kyoko Kuwahara-Arai², Akira Uchiyama¹, Kazuyoshi Kon¹, Hironao Okubo³, Shunhei Yamashina¹, Kenichi Ikejima¹, Shigehiro Kokubu⁴, Akihisa Miyazaki³ and Sumio Watanabe¹

The liver has an immune tolerance against gut-derived products from the portal vein (PV). A disruption of the gut–liver axis leads to liver injury and fibrosis. The spleen is connected to the PV and regulates immune functions. However, possible splenic effects on liver fibrosis development are unclear. Lipocalin-2 (Lcn2) is an antimicrobial protein that regulates macrophage activation. To clarify the role of the spleen in liver fibrosis development, we induced liver fibrosis in mice after splenectomy, and investigated liver fibrosis development. Liver fibrosis resulted in significantly increased splenic Lcn2 levels, but all other measured cytokine levels were unchanged. Splenectomized mice showed enhanced liver fibrosis and inflammation accompanied by significantly decreased Lcn2 levels in PV. Lipopolysaccharide-stimulated primary Kupffer cells, resident liver macrophages, which were treated with recombinant Lcn2 (rLcn2) produced less tumor necrosis factor- α and Ccl2 and the activation of hepatic stellate cells, the effector cells for collagen production in the liver, was suppressed by co-culture with rLcn2-treated Kupffer cells. In addition, the involvement of gut-derived products in splenectomized mice was evaluated by gut sterilization. Interestingly, gut sterilization blocked the effect of splenectomy on liver fibrosis development. In conclusion, spleen deficiency accelerated liver fibrosis development and decreased PV Lcn2 levels. The mechanism of splenic protection against liver fibrosis development may involve the splenic Lcn2, triggered by gut-derived products that enter the liver through the PV, regulates Kupffer cells activated by the gut–liver axis. Thus, the splenic Lcn2 may have an important role in regulating the immune tolerance of the liver in liver fibrosis development.

Laboratory Investigation (2017) 97, 890–902; doi:10.1038/labinvest.2017.44; published online 15 May 2017

Liver fibrosis is caused by chronic exposure to different insults such as exposure to viruses, alcohol or metabolic syndrome.¹ The liver has immune tolerance against foreign antigens such as gut-derived products, including lipopolysaccharides (LPSs) through the portal vein (PV). A disruption of gut–liver axis impaired the barrier function of the gut and immunological responses in the liver is closely related to a variety of liver injuries, and the development of liver fibrosis.²

The spleen is linked to the liver by PV and also a part of the portal venous system. The general functions of the spleen are assumed to be clearance of particulates from the blood, induction of immune responses, and generation of cellular components of blood. However, the precise function of the

spleen has been elusive.³ Splenomegaly due to immune hyperplasia or disordered immune regulation is often found in infectious or inflammatory disease.³ Hence, palpation of the spleen is a routine and important component of physical examinations.⁴ The portal venous system consists of the hepatic portal (liver), splenic (spleen) and superior mesenteric (gut) veins. Anatomically, only the spleen and the gut are connected to the portal venous system. Other organs are directly linked to the systemic circulation. It is hypothesized that immune reactions against gut-derived products in the liver could be affected by cytokines produced by the spleen connected through the portal venous system. In other words, what happening in the spleen may have an impact on

¹Department of Gastroenterology, Juntendo University School of Medicine, Tokyo, Japan; ²Department of Microbiology, Juntendo University School of Medicine, Tokyo, Japan; ³Department of Gastroenterology, Juntendo University Nerima Hospital, Tokyo, Japan and ⁴Institute for Liver Disease Minimal Invasive Treatment, Shin-Yurigaoka, General Hospital, Kanagawa, Japan

Correspondence: Dr T Aoyama, MD, PhD, Department of Gastroenterology, Juntendo University School of Medicine, 2-1-1 Hongo, Bunkyo-ku, Tokyo 113-8471, Japan or Department of Gastroenterology, Juntendo University Nerima Hospital, Tokyo, Japan, 3-1-10 Takanodai, Nerima-ku, Tokyo 177-8521, Japan or Institute for Liver Disease Minimal Invasive Treatment, Shin-Yurigaoka, General Hospital, Kanagawa, Japan, 255 Furusawatoko, Asao-ku, Kawasaki-shi, Kanagawa 215-0026, Japan.
E-mail: aoyama@juntendo.ac.jp

Received 12 September 2016; revised 25 March 2017; accepted 31 March 2017

gut–liver axis. Although the spleen and liver display related immune reactions, it is generally accepted that splenomegaly found in patients with cirrhosis is mainly caused by congestion owing to portal hypertension.⁵ Whether congestion is the only reason for splenomegaly during the development of liver fibrosis is yet to be validated.

Kupffer cells are known as resident liver macrophages and are located in the sinusoids, which provide an entrance to the liver and are directly connected to the PV. Kupffer cells have a pivotal role in maintaining immune tolerance,⁶ although they are exposed to various molecules, including cytokines from the gut and spleen through PV. During liver injury, increased levels of LPS in PV is a consequence of increased permeability of the intestinal mucosal barrier.² LPS-stimulated Kupffer cells promote activation of the hepatic stellate cells (HSCs), the major cell populations involved in the production of extracellular matrix protein during liver fibrosis.⁷ Thus, Kupffer cell regulation is an important target for preventing the development of liver fibrosis.⁸

Lipocalin-2 (Lcn2) is an antimicrobial protein that scavenges a subset of bacterial siderophores, and suppresses bacterial growth.⁹ Lcn2 is expressed in the red pulp of the spleen,¹⁰ and is reported to have an important role in protecting against malaria infection.¹¹ In addition, Lcn2 has been shown to regulate macrophage activation in several experimental models such as a high-fat diet, pneumococcal pneumonia and neurological disorders.^{12–14} In this study, we investigated the role of the spleen in the development of carbon tetrachloride (CCl₄)- or thioacetamide-induced mouse liver fibrosis, with a focus on splenic cytokine expression, including that of Lcn2. Finally, to assess the interaction of gut–liver axis and spleen, we examined the effect of gut sterilization in the development of liver fibrosis in splenectomized mice.

MATERIALS AND METHODS

Animal Model of Splenectomy and Liver Fibrosis

Specific pathogen-free, male wild-type (WT) C57BL/6J mice (Jackson Laboratories) were used. Splenectomy or a sham surgery was performed at 7 weeks after birth. For the CCl₄-induced liver fibrosis model, 1 week after surgery, mice were injected intraperitoneally with CCl₄ diluted 1:3 in olive oil (Wako), or with vehicle alone (olive oil) at a dose of 0.5 µl/g of body weight twice a week for a total of 12 injections.¹⁵ For the thioacetamide-induced liver fibrosis model, 1 week later surgery, male WT mice were given repeated intraperitoneal injections of thioacetamide (three times per week; 0.1 mg/g body weight for the initial week and 0.2 mg/g body weight for subsequent weeks) for up to 5 weeks.¹⁶ Mice were killed 48 or 24 h after the last CCl₄ or thioacetamide injection, respectively. Blood samples were collected from the inferior vena cava and PV by 27G needle. The mice received humane care according to the National Institutes of Health recommendations outlined in Guide for the Care and Use of Laboratory Animals. All animal

experiments were approved by the institutional animal care and use committees of Juntendo University, Tokyo, Japan.

Gut Sterilization

Mice were treated with ampicillin (1 g/l; Sigma), neomycin sulfate (1 g/l; CalBiochem), metronidazole (1 g/l; Sigma) and vancomycin (500 mg/l; Wako) in drinking water for 3 weeks. This treatment was followed by splenectomy and CCl₄ or vehicle intraperitoneal injections were then started 1 week after the surgery. Antibiotic treatment was continued until the mice were killed.^{17,18} To validate gut sterilization, we followed the protocol of reference number 17. Briefly, fecal matter was removed from colons using sterile technique, placed in conical tubes with thyoglycolate, weighed and vortexed until homogenous. Contents were diluted and plated on sheep blood medium agar plates for the growth of anaerobes and aerobes. Colonies were counted after incubation at 37 °C for 48 h (aerobes) and 72 h (anaerobes)¹⁷ (Supplementary Figure S1).

Histological Analysis

For immunohistochemical analysis, liver or spleen specimens were fixed in 10% buffered formalin and were incubated with a monoclonal antibody against α -smooth muscle actin (α -SMA; Sigma) with an M.O.M. kit (Vector Laboratories), rat anti-mouse F4/80 (eBioscience) and rat anti-mouse Gr1 (eBioscience). 3,3'-Diaminobenzidine,tetrahydrochloride (DAB)-positive cells were counted in five 100 × fields on each slide to determine the average number. The percentage of DAB-positive cells in total nucleated cells was measured. In the spleen specimens, we measured the percentage of DAB-positive cells in total nucleated cells located in the red pulp. Specimens were observed and photographed using a microscope equipped with a digital imaging system (Leica DM 2000, Leica Microsystems). For immunofluorescent staining, tissue sections were incubated with an antibody to Gr1 (eBioscience) or Lcn2 (R&D Systems) followed by imaging with fluorescent microscopy (BZ-9000, KEYENCE). Gr1 and Lcn2-positive cells were counted 200 × fields on each slide to determine the average number. In the spleen specimens, the percentage of Gr1 and Lcn2-positive cells/total nucleated cell in the red pulp was measured. For measuring sirius red-positive area, we used Image J version 1.47v.

Western Blot

The preparation of whole-cell protein extracts from frozen livers or spleens, and subsequent immunoblotting were performed as previously described.¹⁹ Blots were incubated with a mouse antibody to α -SMA and β -actin (Sigma) and then were visualized using the enhanced chemiluminescence light method (GE Healthcare).

Enzyme-Linked Immunosorbent Assay

Lcn2 concentrations in the spleen, liver and PV were determined using an enzyme-linked immunosorbent assay

(ELISA) kits (R&D Systems) according to the manufacturer's instruction.²⁰

Hydroxyproline Assay

Hepatic hydroxyproline content was measured by using Hydroxyproline assay kit (QuickZyme Biosciences) according to the manufacturer's instruction.

Quantitative Real-Time Polymerase Chain Reaction

Total RNA was prepared from cells or frozen liver tissues using TRIzol reagent (Invitrogen) or the Illustra RNAspin Mini RNA Isolation kit (GE Healthcare), respectively. RNA was reverse transcribed using a high-capacity complementary DNA reverse-transcription kit (Applied Biosystems). Quantitative real-time PCR was performed using the 7500 Fast Real-time polymerase chain reaction (PCR) System (Applied Biosystems). PCR primer sequences for these reactions are listed in Supplementary Table S1. The expression of the respective genes was normalized to Gapdh RNA as an internal control. For Kupffer cell experiments, Rpl4 RNA was used as an internal control for normalization.²¹

Isolation of Hepatocytes, Kupffer Cells and HSCs

WT mice were treated with intraperitoneal injections of CCl₄ or vehicle twice a week for a total of four injections. To isolate Kupffer cells, collagenase–pronase perfusion was performed, followed by 14.5% Nycodenz (Histodenz; Sigma) gradient centrifugation and subsequent positive selection of CD11b-expressing cells by magnetic antibody cell sorting (MACS; Miltenyi Biotech) as described by the manufacturer.¹⁵ Kupffer cells isolated from WT mice were cultured in Roswell Park Memorial Institute 1640 (RPMI-1640) medium (Invitrogen) containing 10% fetal bovine serum (FBS). After 24 h of incubation, the medium was changed into an RPMI-1640 medium containing 1% FBS, and the cells were then incubated with 150 ng/ml recombinant Lcn2 (rLcn2; R&D Systems) or phosphate-buffered saline (PBS) vehicle for 6 h more with or without 10 ng/ml LPS (Sigma). HSCs were isolated by digestion with collagenase and pronase, followed by gradient centrifugation using 8.2% Nycodenz (Histodenz; Sigma) and then CD11b+ Kupffer cells were removed by MACS. An isolated HSC purity of >95% was confirmed by immunostaining with anti-desmin antibody (Neomarkers) as previously described.¹⁵

To isolate hepatocyte, Kupffer cells and HSCs from one mouse, we used two-step collagenase–pronase perfusion followed by three-layer discontinuous density gradient centrifugation with 8.2% and 14.5% Nycodenz (Histodenz; Sigma).²² HSCs were collected between the 0% and 8.2% layer. The Kupffer cell fraction was selected by MACS using anti-CD11b Micro Beads (Miltenyi Biotech).

Measurement of Collagen-Driven GFP Expression in HSCs

To measure collagen promoter activity, HSCs (1×10^5 cells per well) were isolated from collagen promoter-driven GFP transgenic mice (pCol9GFPHS4,5 transgene).²³ HSCs were incubated with rLcn2 (R&D Systems) or vehicle (PBS) for 48 h. For co-culture experiments, HSCs were co-cultured with Kupffer cells (4×10^5 cells per well) for 48 h in the presence or absence of 150 ng/ml rLcn2 (R&D Systems). Kupffer cells were isolated from WT mice treated with or without CCl₄. Isolated Kupffer cells were put in transwell insert, and primary HSCs from collagen promoter-driven GFP transgenic mice were put in lower well. The number of GFP-positive cells was determined via the counting of GFP-positive cells and total cells in 10 randomly chosen high-power fields¹⁵ viewed with fluorescent microscopy (BX-X710, KEYENCE).

Statistical Analysis

Data are expressed as the mean \pm s.e.m. Statistical differences between means were determined using Student's *t*-tests or analysis of variance on ranks, followed by a *post-hoc* test (Student–Newman–Keuls all pairwise comparison procedures), as appropriate. *P*-values <0.05 were considered statistically significant.

RESULTS

Nucleated Cell Numbers are Increased in the Red Pulp of the Spleen of Mice with CCl₄-Induced Liver Fibrosis

To investigate spleen morphological changes associated with mouse liver fibrosis, we evaluated spleen macroscopic features and weights following CCl₄ treatment. Spleens were visibly enlarged (Figure 1a), and mean spleen weight from CCl₄-treated mice was 1.73-fold heavier than that from control (vehicle-treated) mice (Figure 1b). Microscopically, splenic red pulp was dilated by congestion, but we also detected an increase up to 25% in the number of nucleated cells in the splenic red pulp following CCl₄ treatment. In contrast, the size of the splenic white pulp was reduced after CCl₄ treatment (Figure 1c). Therefore, not only congestion, but also an increase in nucleated cells was evident in splenomegaly in the CCl₄-induced mouse liver fibrosis models.

Lcn2 Expression is Increased in the Spleen of Mice with CCl₄-Induced Liver Fibrosis

To examine the hypothesis that spleen produces several cytokines during the development of liver fibrosis, we measured mRNA expression of pro- and anti-inflammatory cytokines, including tumor necrosis factor- α (Tnf- α), Ccl2, interleukin-6 (Il-6), arginase-1 and Il-10 in the spleens of CCl₄- or vehicle-treated mice. Notably, levels of all measured cytokines, except Lcn2, were not significantly different between the two groups; however, splenic Lcn2 mRNA levels were 35-fold higher in the CCl₄-treated than in the vehicle-treated group (Figure 2a). Similar results were obtained in

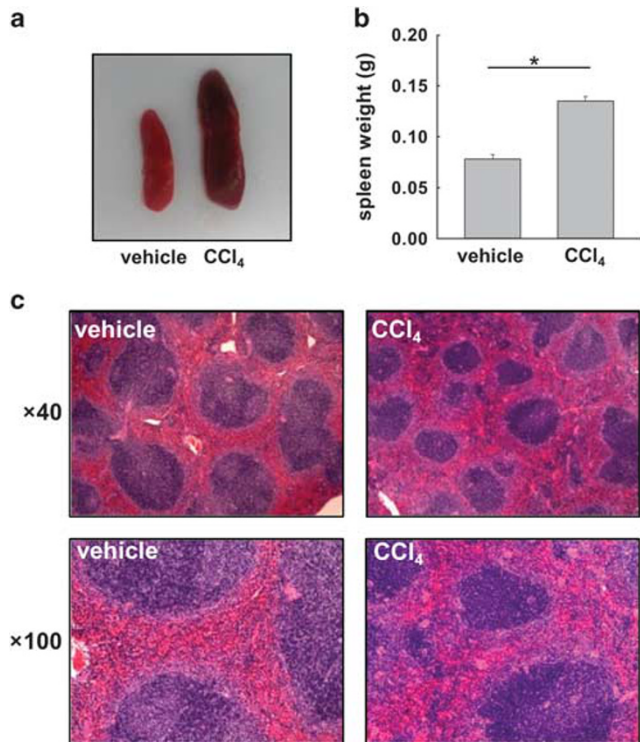


Figure 1 Nucleated cell numbers are increased in the red pulp of the spleen of mice with CCl₄-induced liver fibrosis. (a) Macroscopic findings of the spleen. (b) Spleen weight. (c) Spleen histology of CCl₄ or vehicle-treated WT mice was assessed by hematoxylin and eosin staining. Upper panels (original magnification $\times 40$), lower panels (original magnification $\times 100$). ($n = 5$), $*P < 0.05$.

another model of mouse liver fibrosis induced by thioacetamide (Supplementary Figure S2). In addition, we measured Lcn2 protein levels in the spleen by ELISA. Splenic Lcn2 protein levels were significantly elevated following CCl₄ treatment compared with that in the vehicle treatment group (Figure 2b). These results indicate strong induction of Lcn2 mRNA and protein expression in the spleen during CCl₄-induced development of mouse liver fibrosis.

Number of Gr1-Positive Cells Expressing Lcn2 is Increased in the Spleen of Mice with CCl₄-Induced Liver Fibrosis

As Gr1-positive cells are reported to express Lcn2,¹¹ we examined the number of Gr1-positive cells in the spleen by immunohistochemistry. Results indicated that number of Gr1-positive cells was significantly increased in the red pulp of the spleen following CCl₄ treatment (Figures 3a and b). Next, we investigated Lcn2 expression in Gr1-positive cells by immunofluorescence. Almost all Gr1-positive cells showed co-expression of Lcn2, and these double-positive cells were significantly more abundant in the red pulp of the spleens from CCl₄-treated mice than in the control mice treated with vehicle (Figures 3c and d). These results indicate that splenomegaly associated with CCl₄-induced liver fibrosis

shows increased number of Gr1-positive cells expressing Lcn2 in the red pulp.

Spleen Deficiency Accelerates the Development of Liver Fibrosis

To investigate the role of the spleen in the development of liver fibrosis, we performed splenectomy or sham surgery before induction of liver fibrosis by CCl₄ treatment. Fibrillar collagen deposition was significantly increased in splenectomized mice compared with that in the sham-operated mice following CCl₄ treatment (Figures 4a and b). Similar results were observed in another model of mouse liver fibrosis induced by thioacetamide (Supplementary Figure S3). To evaluate HSC activation, we examined α -SMA expression in the liver. Hepatic α -SMA expression was enhanced in splenectomized mice compared with that in the sham-operated control mice, as assessed by immunohistochemistry and western blotting (Figures 4c and d). The hydroxyproline content in the liver was significantly increased in the splenectomized mice compared with sham-operated mice following CCl₄ treatment (Figure 4e). Similarly, the expression of hepatic fibrotic gene mRNAs, including collagen α (I) 1, tissue inhibitor metalloproteinase 1 (Timp-1) and transforming growth factor- β 1 (Tgf- β 1) were significantly increased in splenectomized mice compared with that in the sham-operated mice following CCl₄ treatment (Figure 4f). These results indicate that spleen deficiency accelerates the development of liver fibrosis.

Spleen Deficiency Augments Liver Inflammation

To further investigate the role of the spleen in liver inflammation, macrophage infiltration and activation were evaluated. F4/80-positive cell numbers were significantly increased in splenectomized mice compared with that in the sham-operated mice after CCl₄ treatment (Figures 5a and b). In addition, quantitative real-time PCR revealed increased expression of CD68, a marker of macrophage activation, in splenectomized mice compared with that in the sham-operated mice post CCl₄ treatment, (Figure 5c). Serum alanine aminotransferase (ALT) levels, serum aspartate aminotransferase (AST) levels and hepatic mRNA expression of inflammatory genes such as Tnf- α and Ccl2 were also significantly increased in splenectomized mice compared with that in the sham-operated mice. However, the hepatic mRNA level of Il-10, an anti-inflammatory gene, was not significantly different between the splenectomized and sham-operated mice following CCl₄ treatment (Figures 5d and e). These results indicate that spleen deficiency enhances Kupffer cell activation and liver inflammation during the development of liver fibrosis.

Decreased Lcn2 Levels in the PV of Splenectomized Mice Treated with CCl₄ Induce Excessive Kupffer Cell Activation

As splenic Lcn2 expression was strongly induced following CCl₄ treatment, we measured Lcn2 levels in PV of mice that

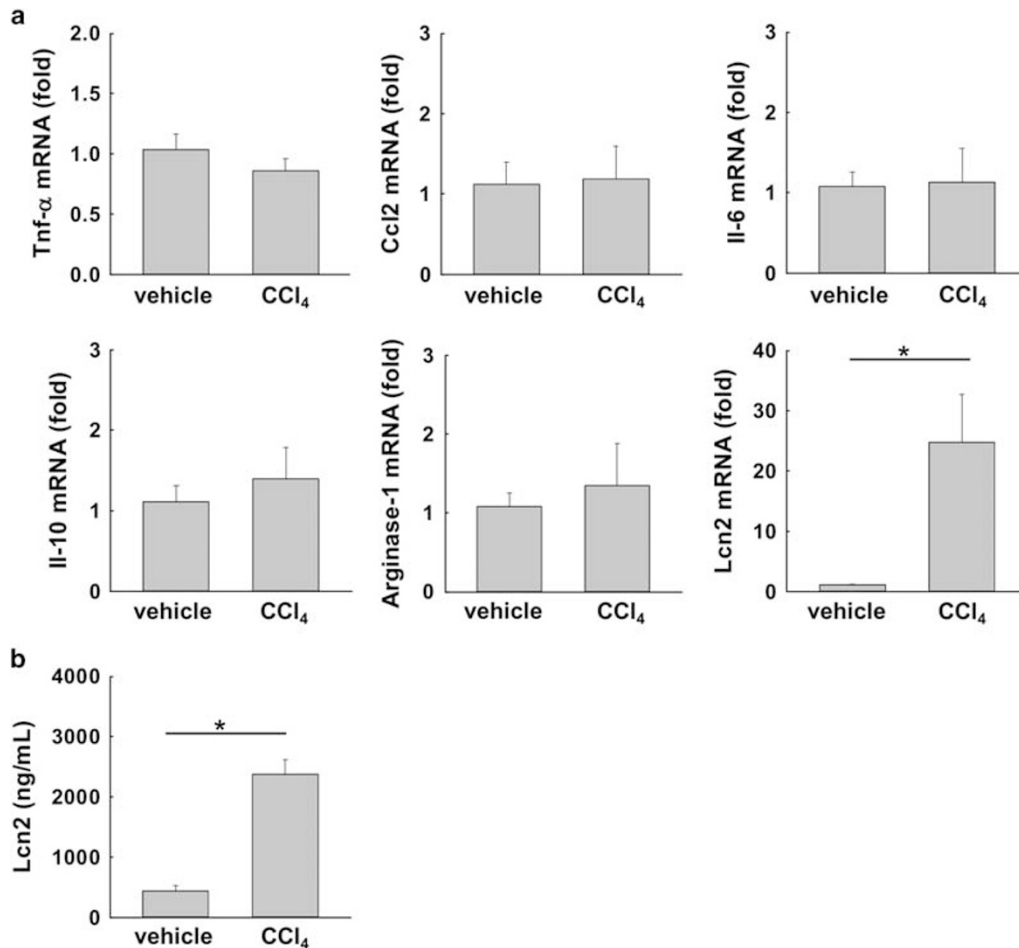


Figure 2 Lcn2 expression is increased in the spleen of mice with CCl₄-induced liver fibrosis. (a) Splenic mRNA levels of Tnf- α , Ccl2, Il-6, Il-10, arginase-1 and Lcn2 were measured by quantitative real-time PCR. (b) Lcn2 levels in the spleen were measured by ELISA. (n = 5), *P < 0.05.

underwent sham surgery or splenectomy before CCl₄ treatment. As expected, the Lcn2 levels in PV after CCl₄ treatment were significantly decreased in splenectomized mice compared with that in the sham-operated mice. However, Lcn2 levels in the liver were slightly increased in the splenectomized mice, but the difference from that in the sham-operated mice was not significant (Figure 6a). As Kupffer cells are located in the sinusoids and are exposed to the portal blood flow directed from PV to the central vein and Lcn2 receptor (Lcn2R) mRNA expression was significantly increased in Kupffer cells isolated from CCl₄-treated mice compared with hepatocytes or HSCs (Supplementary Figure S4), we hypothesized that the decrease in the Lcn2 levels in portal affects Kupffer cell activation. To investigate the role of Lcn2 in PV, we examined the effect of rLcn2 on Kupffer cells stimulated by LPS. As the concentration of Lcn2 in PV differed by approximately 150 ng/ml between the sham-operated and splenectomized mice (Figure 6a), we added 150 ng/ml of rLcn2 to LPS-stimulated Kupffer cells. Notably, Tnf- α and Ccl2 mRNA levels were significantly decreased by rLcn2 treatment of LPS-stimulated Kupffer cells;

however, Il-10 mRNA levels were not changed (Figure 6b). In subsequent experiments, we tested the effect of rLcn2 on HSCs. HSCs isolated from collagen promoter-driven GFP transgenic (collagen-GFP) mice were treated with rLcn2 at different concentrations. HSC collagen α 1(I) promoter activity did not significantly change following incubation with rLcn2 (Figure 6c). In addition, rLcn2 treatment did not alter collagen α 1(I) mRNA expression in HSCs (Figure 6d). These results indicate that rLcn2 does not regulate HSC activation. To test whether exposure of Kupffer cells to rLcn2 affects HSC activation, we co-cultured HSCs isolated from collagen-GFP mice with Kupffer cells isolated from WT mice treated with or without CCl₄ and with or without rLcn2 incubation. Compared with co-culture with CCl₄-treated mice Kupffer cells incubated with vehicle, the number of GFP-positive HSCs significantly decreased when CCl₄-treated mice Kupffer cells incubated with rLcn2 were used for co-culturing (Figures 6e and f). These results indicate that spleen deficiency leads to a decrease in Lcn2 levels in PV, which induces excessive Kupffer cell activation in the liver.

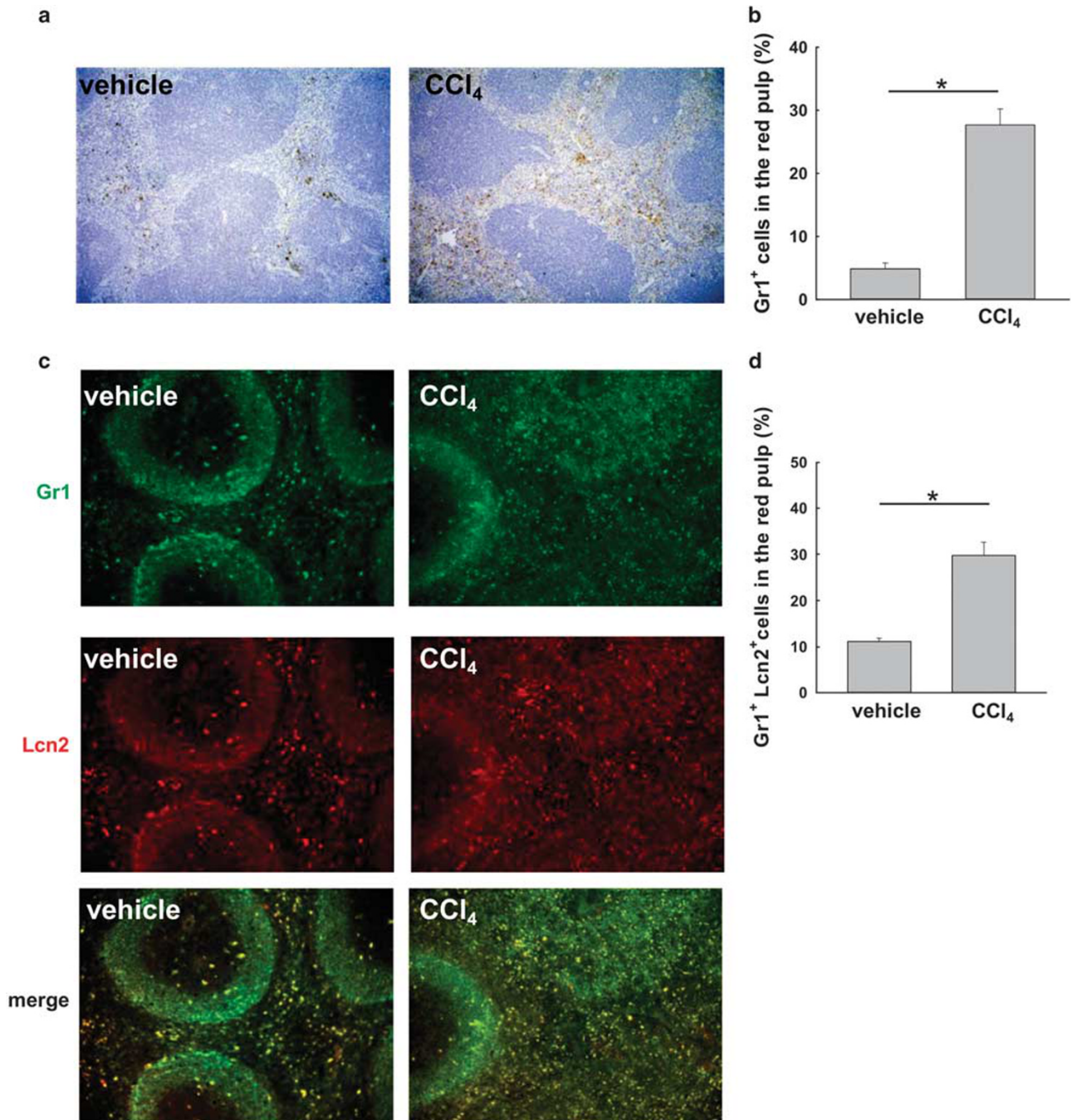


Figure 3 Number of Gr1-positive cells expressing Lcn2 is increased in the spleen of mice with CCl₄-induced liver fibrosis. (a) Immunohistochemistry for Gr1 (original magnification $\times 100$) and (b) its quantification are shown. (c) Gr1 expression (in green) was detected by fluorescence microscopy via containing with Lcn2 (in red) (original magnification $\times 200$) and (d) its quantification. ($n=5$), $*P<0.05$.

Gut Sterilization Neutralizes Accelerated Liver Fibrosis Development in Splenectomized Mice Treated with CCl₄

As Lcn2 is known as an antibacterial protein, and both the spleen and intestines are linked to the portal circulation, we hypothesized that gut-derived products, including bacterial pathogens in the intestine, could be related to the effect of splenectomy in the development of liver fibrosis. To test

this hypothesis, we used an experimental model based on gut sterilization with a cocktail of nonabsorbable broad-spectrum antibiotics.^{17,18} We treated mice with antibiotics and performed splenectomy or sham surgery followed by CCl₄ or vehicle treatments. Following antibiotic-mediated gut sterilization, CCl₄-induced liver fibrosis and macrophage infiltration in splenectomized mice were found to be

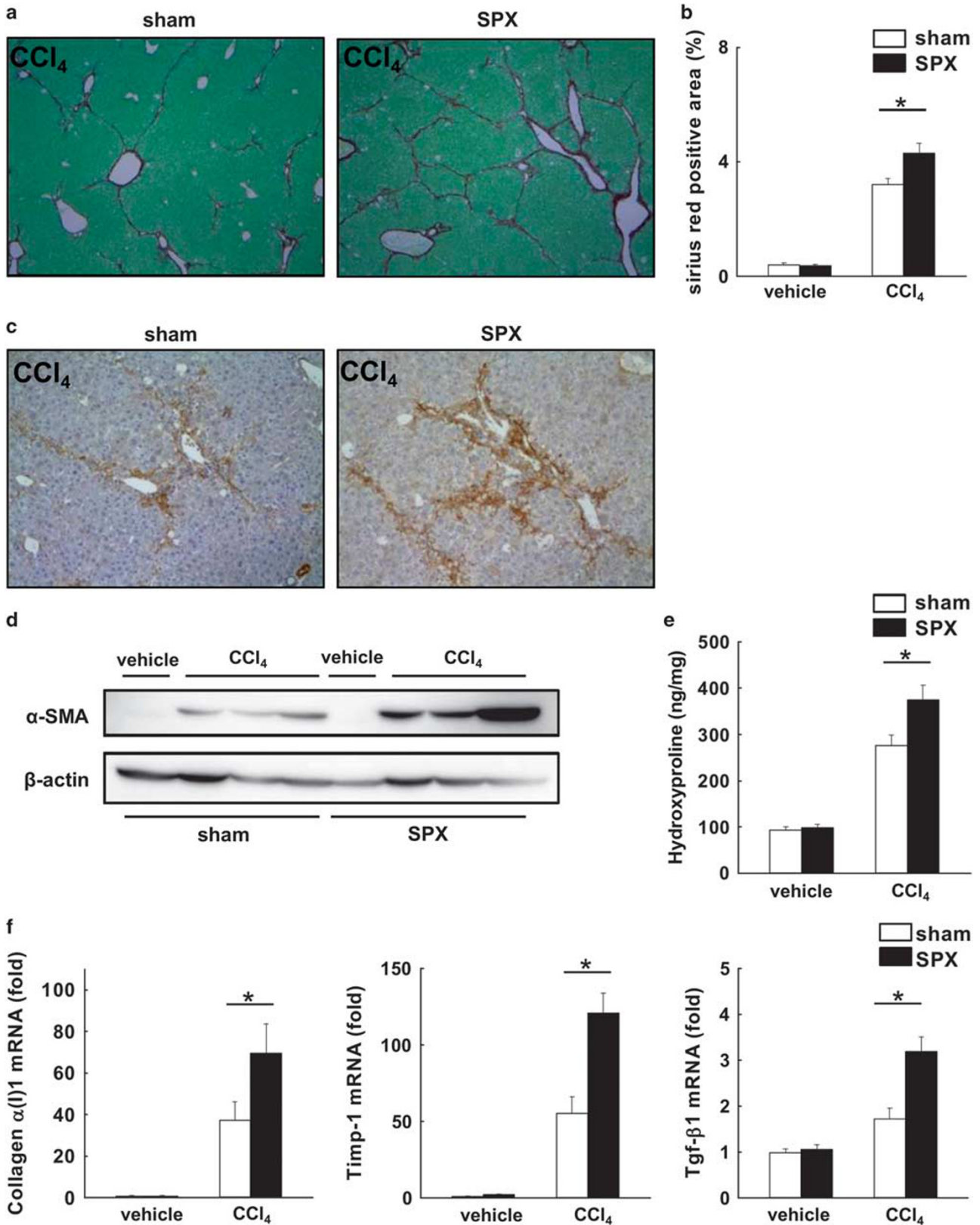


Figure 4 Splenic deficiency accelerates the development of liver fibrosis. (a) Sirius red staining (original magnification $\times 40$) and (b) its quantification are shown. The expression of α -SMA in the liver was detected by (c) immunohistochemistry (original magnification $\times 100$), and (d) western blot. (e) The hydroxyproline content in the liver was measured. (f) Hepatic mRNA expression of Collagen $\alpha 1(I)$, Timp-1 and Tgf- $\beta 1$ mRNA was measured by quantitative real-time PCR. Sham, sham surgery; SPX, splenectomy; ($n = 5$), $*P < 0.05$.

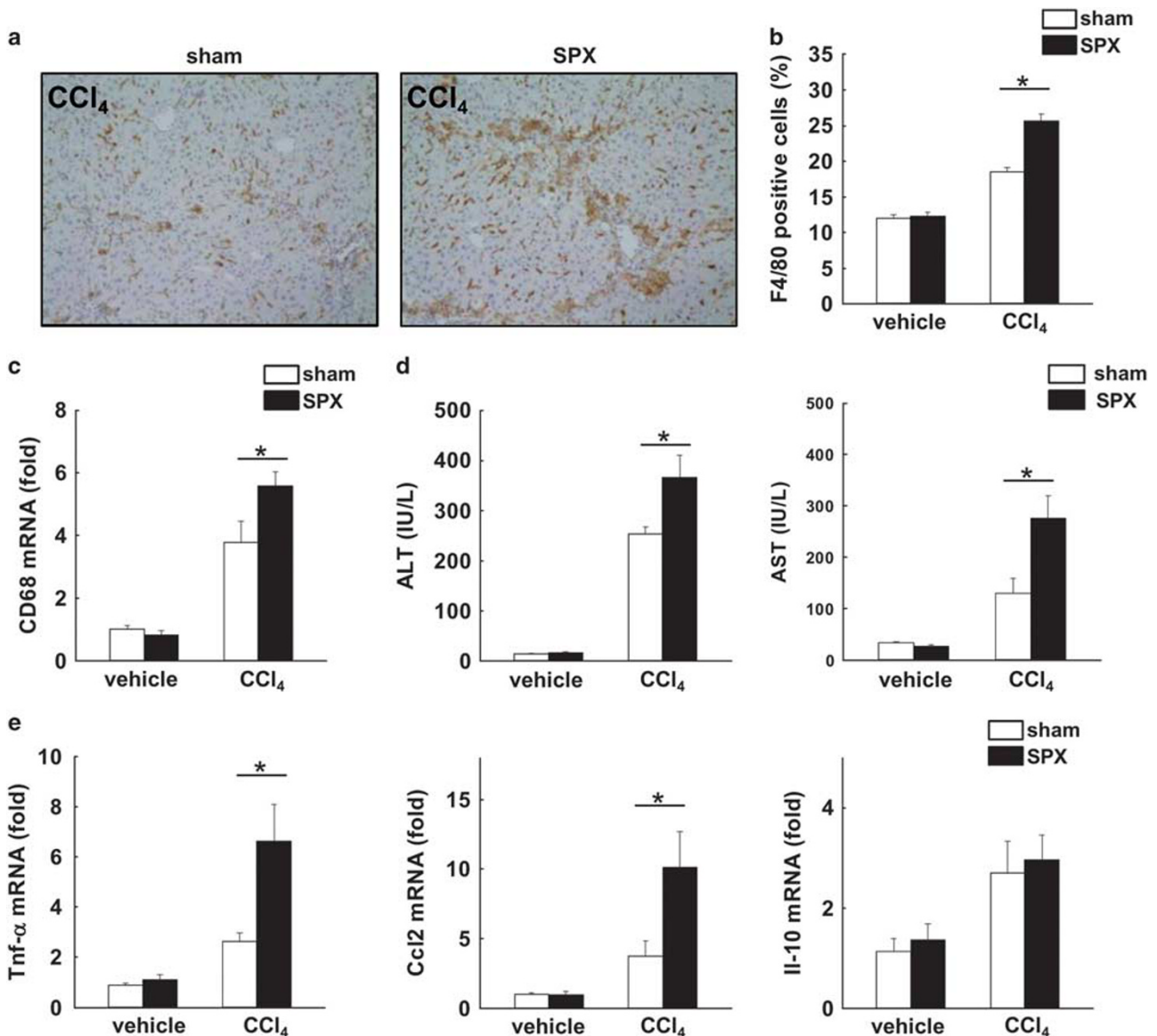


Figure 5 Spleen deficiency augments liver inflammation. Immunohistochemistry for (a) F4/80 and (b) its quantification are shown (original magnification $\times 100$). (c) Hepatic mRNA expression of CD68 was measured by quantitative real-time PCR. (d) Serum ALT and AST levels were measured. (e) Hepatic mRNA expression of Tnf- α , Ccl2 and Il-10 were measured by quantitative real-time PCR. Sham, sham surgery; SPX, splenectomy; ($n=5$), $*P<0.05$.

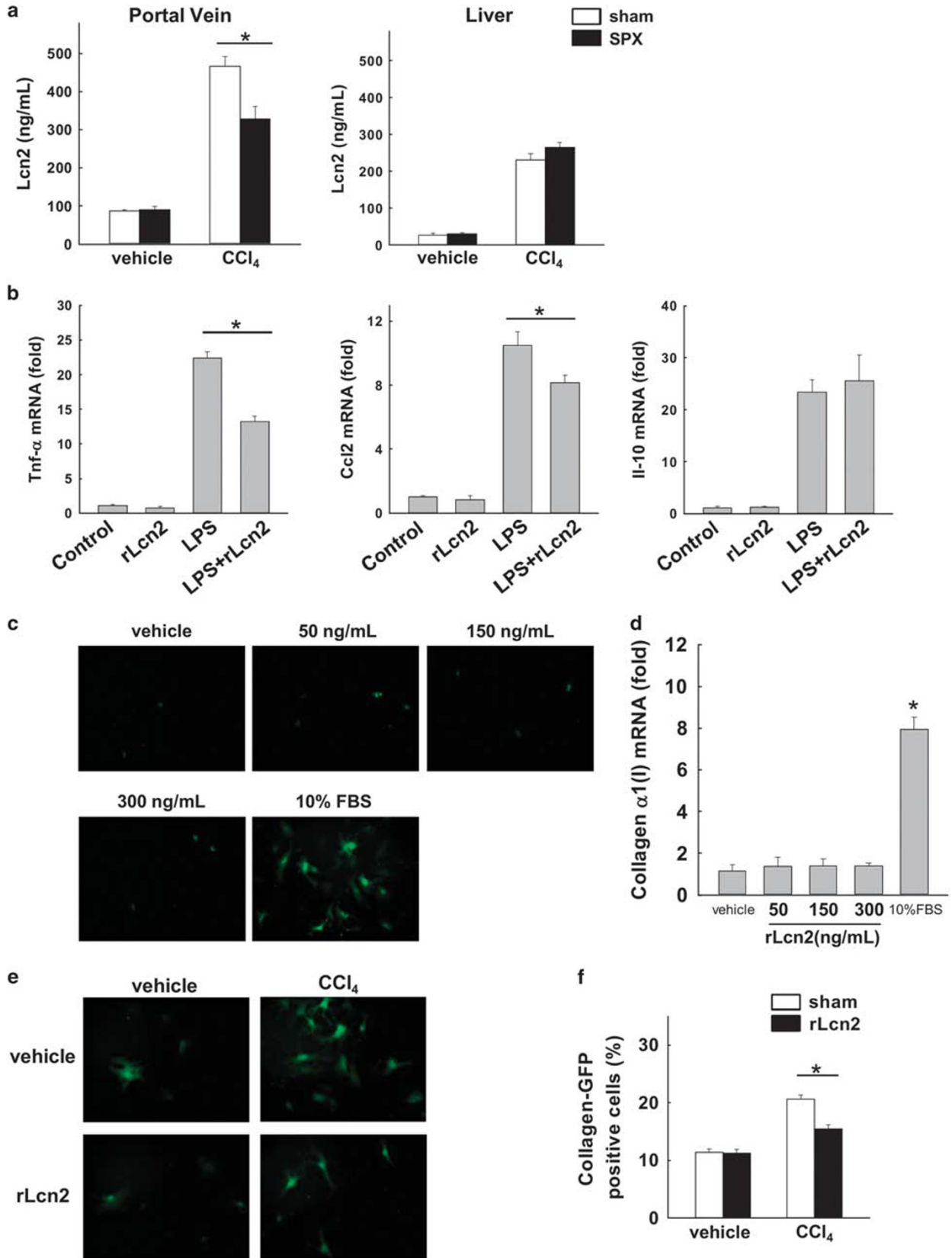
comparable to that in the sham-operated mice (Figures 7a-d). Similarly, hepatic collagen $\alpha 1(1)$, Ccl2 and Tnf- α mRNA levels were not different between the splenectomized and sham-operated mice (Figure 7e). In addition, Lcn2 levels in the PV and the liver of the splenectomized mice after CCl₄ treatment were not significantly different from that in the CCl₄-treated sham-operated mice (Figure 7f).

On the other hand, splenic Lcn2 levels were increased following CCl₄ treatment (Figure 7g); however, the levels were not so high compared with non-gut-sterilized model (Figure 2b). These results indicate that gut sterilization negates the impact of spleen deficiency on the development of liver fibrosis. Thus, this study suggests a protective and

supportive role of spleen in immune tolerance for gut-derived products in the liver during the development of liver fibrosis.

DISCUSSION

Throughout evolution, mammals, including humans, have retained the spleen, most likely because the spleen has critical functions. It is tempting to speculate that as spleen is critical to liver function, evolution has ensured that the spleen is not directly connected to the systemic circulation but to the portal venous system. We propose a possibility that the spleen has a critical role to keep immune tolerance of the liver against gut-derived products during the development of liver fibrosis.



In this study, we demonstrated that splenomegaly associated with CCl₄-induced liver fibrosis in mice involves increased number of Gr1-positive cells that express Lcn2 in the red pulp of the enlarged spleen (Figure 3). In addition, spleen deficiency enhanced the development of liver fibrosis induced by CCl₄ or thioacetamide. The underlying mechanism involves decreased Lcn2 levels in PV because of spleen deficiency, resulting in excessive Kupffer cell activation stimulated by exposure to LPS. As many macrophages are located in the red pulp of the spleen,¹⁰ we initially expected pro- or anti-inflammatory cytokine expression to be altered in the spleen of mice with CCl₄-induced liver fibrosis.²⁴ However, cytokine expression did not change, whereas splenic Lcn2 mRNA and protein expression levels were drastically increased post CCl₄ or thioacetamide treatment (Figure 2a, Supplementary Figure S2). Lcn2 is also known as neutrophil gelatinase-associated lipocalin and was identified as a soluble, secreted protein found in human neutrophil granules.²⁵ Lcn2 has multiple functions related to cell death, cell differentiation, tumorigenesis and hematogenesis.^{26–29} Xu *et al*³⁰ reported that liver is the major source of Lcn2 in systemic bacterial infection and liver regeneration models. In contrast, in this study, we demonstrated that Lcn2 levels in the spleen were drastically increased compared with that in the liver following CCl₄-induced liver fibrosis (Figures 2b and 6a). These results indicated that the induction of Lcn2 is different under each pathological condition. In the development of liver fibrosis, Lcn2 is highly expressed in the spleen but not in the liver. In our study, spleen deficiency led to exaggerated liver inflammation and development of fibrosis accompanied by excessive Kupffer cell activation (Figures 4 and 5). Splenectomized mice with CCl₄-induced liver injury showed decreased levels of Lcn2 in PV (Figure 6a). Anatomically, Kupffer cells are located in the sinusoids, which are the first place for the liver to face portal blood flow. As sinusoidal endothelial cells lose their fenestrations in fibrotic liver¹ and the direction of blood flow in sinusoids is from PV to the central vein, for activation of Kupffer cells, the role of Lcn2 located in the PV is more important than that of Lcn2 in the liver (Figure 6a). Therefore, we hypothesized that Kupffer cell activation is affected by a low concentration of Lcn2 in the PV.

Lcn2 levels did decrease in the portal blood with splenectomy, but did not go to zero. As we showed in Figure 6a, Lcn2 was expressed on the liver. Furthermore, Lcn2 was detected in the kidney in both splenectomized and sham-operated mice (data not shown). However, Lcn2 levels in the

liver and kidney were not changed in each mouse. These results suggest that the compensation by liver or kidney could manage to keep Lcn2 levels in the PV, but this compensation was not complete. Therefore, the Lcn2 levels in the PV were decreased in CCl₄-treated splenectomized mice (Figure 6a).

Several reports show a relationship between Lcn2 and macrophages; however, the effect of Lcn2 varies depending on specific conditions and tissues. Zhang *et al.*³¹ demonstrated that Lcn2 decreased the expression of Tnf- α , MCP-1, Il-1 β and Il-6 in RAW264.7 macrophages stimulated by LPS. Furthermore, Lcn2 increased Il-10 mRNA levels in bone marrow-derived macrophages incubated with *Streptococcus pneumoniae*, which are Gram-positive bacteria.¹³ In contrast, Lcn2 enhanced Tnf- α and Cxcl10 mRNA expression in microglia.¹⁴ In this study, we demonstrated that in LPS-stimulated Kupffer cells, rLcn2 suppressed the expression of Tnf- α and Ccl2 mRNAs, but not Il-10 mRNA expression (Figure 6b). Although exogenous rLcn2 did not affect HSCs directly (Figures 6c and d), co-culture experiments showed that CCl₄-treated mouse Kupffer cells incubated with rLcn2 had a reduced number of collagen-GFP-positive HSCs (Figures 6e and f) compared with CCl₄-treated mouse Kupffer cells incubated with vehicle. The mechanism by which the effects of Lcn2 vary between macrophages and tissues is unknown; however, the present work demonstrates that at least for Kupffer cells, Lcn2 has a role in suppressing excessive Kupffer cell activation.

It is reported that in a mouse model of renal transplantation, rLcn2 treatment ameliorated histological damage and functional impairment in recipient mice through reducing cell apoptosis.³² Although the mechanism of this is not clear, other reports showed that Lcn2 may inhibit cell damage by upregulation of regulatory T cells and induction of T-cell apoptosis.^{33,34} Furthermore, Borkham-Kamphorst *et al*³⁵ reported that Lcn2 expression on the hepatocytes was induced by Il-1 β , and Lcn2 knock out mice showed more liver damage following chronic CCl₄ treatment. Tnf- α treatment led to elevate cleaved caspase-3 levels in Lcn2 knock out hepatocytes.³⁶ Similarly, exogenous Lcn2 reduced renal tubular cell apoptosis.³⁷ These reports demonstrate that Lcn2 has a protective role in cell damage and support our study.

As the spleen is a source of immune cells, there is a possibility that some immune cells of the spleen those come into the liver may have a role in this model. In this study, we found that Lcn2, which is an antimicrobial protein and expressed on Gr1-positive cells, tremendously increased in the

Figure 6 Decreased Lcn2 levels in the PV of splenectomized mice treated with CCl₄ induce excessive Kupffer cell activation. (a) Lcn2 levels in the PV and the liver. (n=5). (b) Tnf- α , Ccl2 and Il-10 mRNA levels of Kupffer cells. (n=4). (c) HSCs isolated from collagen-GFP mice were incubated with rLcn2 or vehicle. Representative photographs were shown (original magnification $\times 200$). (n=4). (d) Collagen $\alpha 1(i)$ mRNA levels of HSCs. (n=4). (e) Collagen-GFP HSCs were co-cultured with Kupffer cells presence or absence of rLcn2 (150 ng/ml). Representative photographs were shown (original magnification $\times 200$). (f) Their quantification. Similar results were obtained in three independent experiments. *P<0.05.

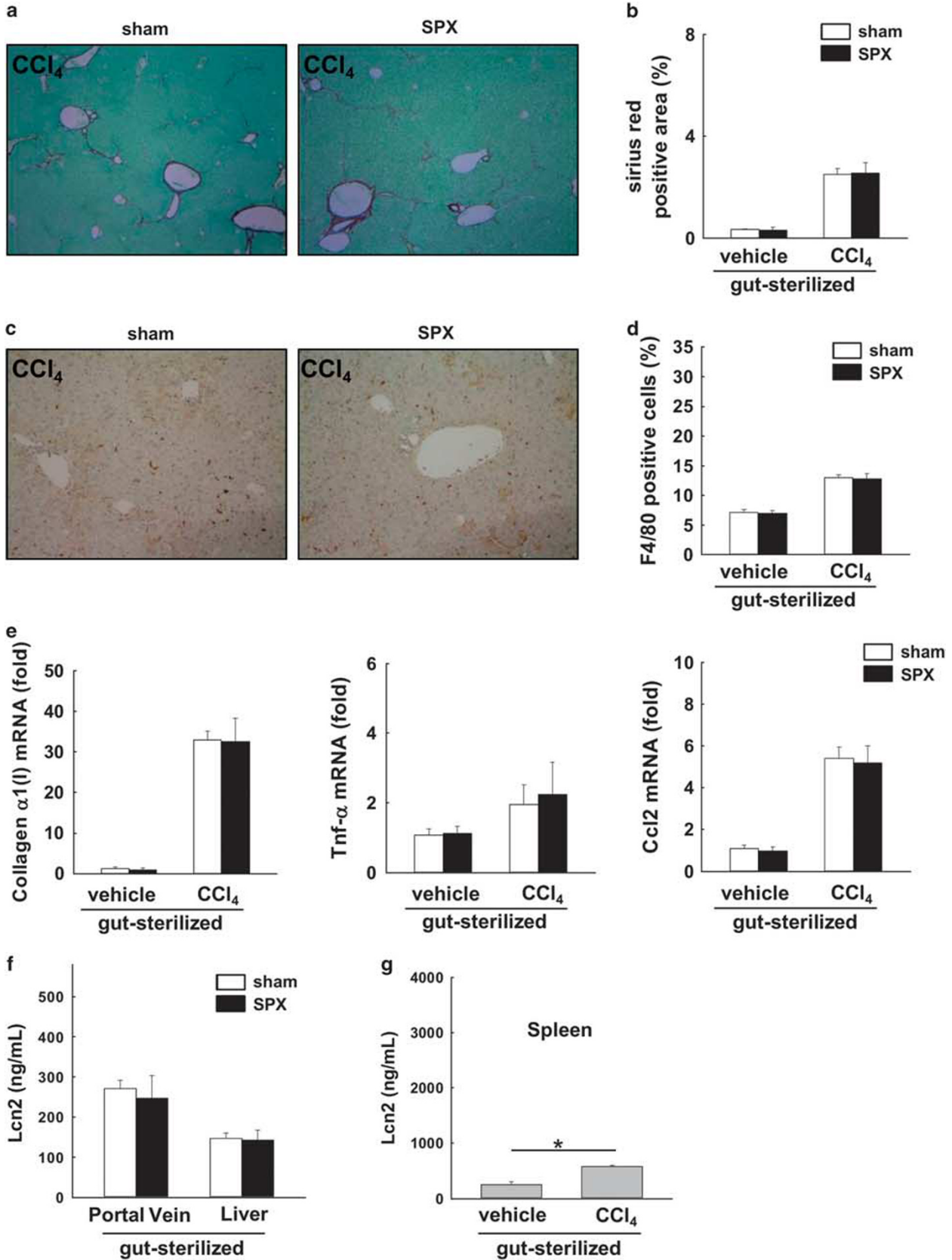


Figure 7 Gut sterilization neutralizes accelerated liver fibrosis development in splenectomized mice treated with CCl₄. **(a)** Sirius red staining (original magnification ×40) and **(b)** its quantification. Immunohistochemistry for **(c)** F4/80 and **(d)** its quantification (original magnification ×100). **(e)** Hepatic mRNA expression of Collagen α1(I), Tnf-α and Ccl2 were measured by quantitative real-time PCR. **(f)** Lcn2 levels in the PV and the liver and **(g)** Lcn2 levels in the spleen were measured by ELISA. (n = 5), *P < 0.05.

spleen with liver fibrosis (Figures 2 and 3). Therefore, we focused on the role of splenic Lcn2 in liver fibrosis development. To assess the possibility that splenic Gr1-positive cells come into the liver in this model, we evaluated the number of Gr1-positive cells in the liver. The number of Gr1-positive cells in the liver was not significantly different between sham-operated and splenectomized mice after CCl₄ treatment (Supplementary Figure S5). In addition, this study also showed that gut sterilization reduced splenic Lcn2 expression and blocked the effect of splenectomy on liver fibrosis development (Figure 7). Therefore, the splenic Lcn2 production induced by gut-derived products has a key role in the liver fibrosis development (Supplementary Figure S6).

Previous experimental studies have shown that splenectomy attenuates liver fibrosis;^{38–40} however, in all of those studies, splenectomies were performed after the development of liver fibrosis. Once liver fibrosis is developed, many collateral pathways, including hepatopetal and hepatofugal flows around PV, also develop because of portal hypertension.⁴¹ Therefore, when splenectomy is performed in fibrotic liver models, severe hemodynamic changes in the hepatopetal flow may occur in the portal venous system, which is related to the liver, especially in the blood flow of sinusoids. In this study, as we wanted to determine the role of the spleen during the development of liver fibrosis, we performed either splenectomy or sham operations before the induction of liver fibrosis by CCl₄ treatment 1 week post-surgery. As hepatopetal collateral blood flow was similar in both splenectomy and sham surgery groups during the development of liver fibrosis, this protocol can minimize the effect of hemodynamic changes in hepatopetal blood flow after splenectomy. In addition, gut sterilization before splenectomy or sham surgery led to comparable levels of hepatic collagen deposition during CCl₄-induced liver fibrosis development in both the sham-operated and splenectomized mice (Figures 7a and b) and similar Lcn2 levels in PV of both groups (Figure 7f). Thus, the effect of splenectomy on the development of liver fibrosis was mainly associated with immunological responses against gut-derived products rather than with hemodynamic changes (Supplementary Figure S6).

Overall, we have presented data supporting a protective role of spleen against a disruption of gut–liver axis during the development of liver fibrosis in mouse experimental models. The splenic Lcn2, triggered by gut-derived products that enter the liver through the PV, regulates Kupffer cells activated by the gut–liver axis. In this study, we focused on the role of the spleen during the development of liver fibrosis and demonstrated the basis for splenomegaly being associated with liver

fibrosis. Further experiments will be required to determine additional functions of the spleen during the development of liver fibrosis. Our study identifies the spleen as a new target for therapeutic intervention in liver fibrosis.

Supplementary Information accompanies the paper on the Laboratory Investigation website (<http://www.laboratoryinvestigation.org>)

ACKNOWLEDGMENTS

We greatly appreciate Dr David A Brenner (University of California, San Diego) for giving us collagen promoter-driven GFP transgenic mice and thank Ms Kumiko Arai (Department of Gastroenterology, Juntendo University School of Medicine) for excellent technical assistance. We also thank Mr Hiroshi Koide, Ms Tomomi Ikeda and Ms Takako Ikegami (Laboratory of Molecular and Biochemical Research, Research Support Center, Juntendo University Graduate School of Medicine) for technical assistance. This work was supported by JSPS KAKENHI grant number 15K19350.

DISCLOSURE/CONFLICT OF INTEREST

The authors declare no conflict of interest.

- Battaller R, Brenner DA. Liver fibrosis. *J Clin Invest* 2005;115:209–218.
- Schwabe RF, Seki E, Brenner DA. Toll-like receptor signaling in the liver. *Gastroenterology* 2006;130:1886–1900.
- Longo D, Fauci A, Kasper D, *et al*. *Harrison's Principles of Internal Medicine* 18th edition. McGraw-Hill Professional: New York, NY, 2011.
- Bickley L, Szilagyi PG. *Bates' Guide to Physical Examination and History-Taking*. Lippincott Williams & Wilkins: Philadelphia, PA, 2012.
- Dooley JS, Lok A, Burroughs AK, *et al*. *Sherlock's Diseases of the Liver and Biliary System*. John Wiley & Sons: Hoboken, NJ, 2011.
- Pellicoro A, Ramachandran P, Iredale JP, *et al*. Liver fibrosis and repair: immune regulation of wound healing in a solid organ. *Nat Rev Immunol* 2014;14:181–194.
- Friedman SL. Mechanisms of hepatic fibrogenesis. *Gastroenterology* 2008;134:1655–1669.
- Marra F, Aleffi S, Galastri S, *et al*. Mononuclear cells in liver fibrosis. *Semin Immunopathol* 2009;31:345–358.
- Goetz DH, Holmes MA, Borregaard N, *et al*. The neutrophil lipocalin NGAL is a bacteriostatic agent that interferes with siderophore-mediated iron acquisition. *Mol Cell* 2002;10:1033–1043.
- Mebius RE, Kraal G. Structure and function of the spleen. *Nat Rev Immunol* 2005;5:606–616.
- Zhao H, Konishi A, Fujita Y, *et al*. Lipocalin 2 bolsters innate and adaptive immune responses to blood-stage malaria infection by reinforcing host iron metabolism. *Cell Host Microbe* 2012;12:705–716.
- Guo H, Jin D, Chen X. Lipocalin 2 is a regulator of macrophage polarization and NF-κappaB/STAT3 pathway activation. *Mol Endocrinol* 2014;28:1616–1628.
- Warszawska JM, Gawish R, Sharif O, *et al*. Lipocalin 2 deactivates macrophages and worsens pneumococcal pneumonia outcomes. *J Clin Invest* 2013;123:3363–3372.
- Jang E, Lee S, Kim JH, *et al*. Secreted protein lipocalin-2 promotes microglial M1 polarization. *FASEB J* 2013;27:1176–1190.
- Aoyama T, Inokuchi S, Brenner DA, *et al*. CX3CL1-CX3CR1 interaction prevents carbon tetrachloride-induced liver inflammation and fibrosis in mice. *Hepatology* 2010;52:1390–1400.
- Ishikawa S, Ikejima K, Yamagata H, *et al*. CD1d-restricted natural killer T cells contribute to hepatic inflammation and fibrogenesis in mice. *J Hepatol* 2011;54:1195–1204.

17. Rakoff-Nahoum S, Paglino J, Eslami-Varzaneh F, *et al*. Recognition of commensal microflora by toll-like receptors is required for intestinal homeostasis. *Cell* 2004;118:229–241.
18. Seki E, De Minicis S, Osterreicher CH, *et al*. TLR4 enhances TGF-beta signaling and hepatic fibrosis. *Nat Med* 2007;13:1324–1332.
19. Aoyama T, Paik YH, Watanabe S, *et al*. Nicotinamide adenine dinucleotide phosphate oxidase in experimental liver fibrosis: GKT137831 as a novel potential therapeutic agent. *Hepatology* 2012;56:2316–2327.
20. Aoyama T, Ikejima K, Kon K, *et al*. Pioglitazone promotes survival and prevents hepatic regeneration failure after partial hepatectomy in obese and diabetic KK-A(y) mice. *Hepatology* 2009;49:1636–1644.
21. Cinar MU, Islam MA, Uddin MJ, *et al*. Evaluation of suitable reference genes for gene expression studies in porcine alveolar macrophages in response to LPS and LTA. *BMC Res Notes* 2012;5:107.
22. Iwaisako K, Jiang C, Zhang M, *et al*. Origin of myofibroblasts in the fibrotic liver in mice. *Proc Natl Acad Sci USA* 2014;111:E3297–E3305.
23. Magness ST, Bataller R, Yang L, *et al*. A dual reporter gene transgenic mouse demonstrates heterogeneity in hepatic fibrogenic cell populations. *Hepatology* 2004;40:1151–1159.
24. Martinez FO, Sica A, Mantovani A, *et al*. Macrophage activation and polarization. *Front Biosci* 2008;13:453–461.
25. Kjeldsen L, Johnsen AH, Sengelov H, *et al*. Isolation and primary structure of NGAL, a novel protein associated with human neutrophil gelatinase. *J Biol Chem* 1993;268:10425–10432.
26. Devireddy LR, Teodoro JG, Richard FA, *et al*. Induction of apoptosis by a secreted lipocalin that is transcriptionally regulated by IL-3 deprivation. *Science* 2001;293:829–834.
27. Yang J, Goetz D, Li JY, *et al*. An iron delivery pathway mediated by a lipocalin. *Mol Cell* 2002;10:1045–1056.
28. Lippi G, Meschi T, Nouvenne A, *et al*. Neutrophil gelatinase-associated lipocalin in cancer. *Adv Clin Chem* 2014;64:179–219.
29. Miharada K, Hiroyama T, Sudo K, *et al*. Lipocalin 2-mediated growth suppression is evident in human erythroid and monocyte/macrophage lineage cells. *J Cell Physiol* 2008;215:526–537.
30. Xu MJ, Feng D, Wu H, *et al*. Liver is the major source of elevated serum lipocalin-2 levels after bacterial infection or partial hepatectomy: a critical role for IL-6/STAT3. *Hepatology* 2015;61:692–702.
31. Zhang J, Wu Y, Zhang Y, *et al*. The role of lipocalin 2 in the regulation of inflammation in adipocytes and macrophages. *Mol Endocrinol* 2008;22:1416–1426.
32. Ashraf MI, Schwelberger HG, Brendel KA, *et al*. Exogenous lipocalin 2 ameliorates acute rejection in a mouse model of renal transplantation. *Am J Transplant* 2016;16:808–820.
33. La Manna G, Ghinatti G, Tazzari PL, *et al*. Neutrophil gelatinase-associated lipocalin increases HLA-G(+)/FoxP3(+) T-regulatory cell population in an *in vitro* model of PBMC. *PLoS ONE* 2014;9:e89497.
34. Floderer M, Prchal-Murphy M, Vizzardelli C. Dendritic cell-secreted lipocalin2 induces CD8+ T-cell apoptosis, contributes to T-cell priming and leads to a TH1 phenotype. *PLoS ONE* 2014;9:e101881.
35. Borkham-Kamphorst E, Drews F, Weiskirchen R. Induction of lipocalin-2 expression in acute and chronic experimental liver injury moderated by pro-inflammatory cytokines interleukin-1beta through nuclear factor-kappaB activation. *Liver Int* 2011;31:656–665.
36. Borkham-Kamphorst E, van de Leur E, Zimmermann HW, *et al*. Protective effects of lipocalin-2 (LCN2) in acute liver injury suggest a novel function in liver homeostasis. *Biochim Biophys Acta* 2013;1832:660–673.
37. An S, Zang X, Yuan W, *et al*. Neutrophil gelatinase-associated lipocalin (NGAL) may play a protective role against rats ischemia/reperfusion renal injury via inhibiting tubular epithelial cell apoptosis. *Ren Fail* 2013;35:143–149.
38. Akahoshi T, Hashizume M, Tanoue K, *et al*. Role of the spleen in liver fibrosis in rats may be mediated by transforming growth factor beta-1. *J Gastroenterol Hepatol* 2002;17:59–65.
39. Morinaga A, Ogata T, Kage M, *et al*. Comparison of liver regeneration after a splenectomy and splenic artery ligation in a dimethylnitrosamine-induced cirrhotic rat model. *HPB (Oxford)* 2010;12:22–30.
40. Yada A, Iimuro Y, Uyama N, *et al*. Splenectomy attenuates murine liver fibrosis with hypersplenism stimulating hepatic accumulation of Ly-6C (I_o) macrophages. *J Hepatol* 2015;63:905–916.
41. Sharma M, Rameshbabu CS. Collateral pathways in portal hypertension. *J Clin Exp Hepatol* 2012;2:338–352.